

Removal of anionic dyes by silica-chitosan composite in single and binary systems: Valorization of shrimp co-product “Crangon-Crangon” and “Pandalus Borealis”

H. El Fargani¹, R. Lakhmiri^{1*}, H. El Farissi¹, A. Albourine², M. Safi³, O. Cherkaoui⁴

1. Laboratory of Materials and Valorization of the Resources, Faculty of Sciences and Techniques of Tangier, Abdelmalek Essaâdi University, Km 10 route de Ziaten, BP 416 Tangier, Morocco.

2. Laboratory of Materials and Environment, Team of Coordination Chemistry, Faculty of Sciences, Ibn Zohr University, BP 8106, 80000 Agadir, Morocco.

3. Laboratory of Physical Chemistry and Bio-Organic Chemistry, URAC 22 University of Hassan II Mohammedia-Casablanca, Faculty of Sciences and Techniques-Mohammedia, BP 146, Mohammedia, Morocco

4. Higher School of Textile and Clothing Industries, Laboratory REMTEX, Casablanca, Morocco.

Received 20 Jun 2016,

Revised 17 Oct 2016,

Accepted 23 Oct 2016

Keywords

- ✓ Chitosan-Silica Composite;
- ✓ Adsorption;
- ✓ Reactive Red 23;
- ✓ Reactive Blue 19;
- ✓ Binary system

R Lakhmiri

lakhmirir@yahoo.fr

+212 661427257

Abstract

In this work, we study the elimination of two anionic dyes (Reactive Red 23 and Reactive Blue 19) in single and binary systems of dyes by adsorption on silica-chitosan composite (Si-Cs). This study focuses on the effectiveness of our Si-Cs composite synthesized chemically by the extraction of chitosan from shrimp « Pandalus Borealis » and « Crangon-Crangon » co-products by the hydrothermo-chemical technique. The composite obtained was characterized by infrared spectroscopy (FT-IR), X-ray diffraction (XRD), scanning electron microscope (SEM) and energy dispersive X-ray analysis (EDXA). The Si-Cs composite was found to have excellent dyes adsorption capacity in both single and binary system of dyes. Batch experiments were carried out for adsorption kinetics, isotherms and thermodynamics. Operational parameters studied were pH, contact time, temperature, dye and adsorbent concentrations. Dyes elimination percentage was between 89% and 97% in both systems, with an optimal contact time of 180min. Equilibrium data agreed well with the Freundlich isotherm model. While the kinetics and thermodynamics parameters were used to establish the adsorption mechanism, the pseudo-second-order kinetic model has presented the best fitting; Thermodynamic studies revealed that the nature of adsorption is not spontaneous and exothermic with a physical adsorption.

1. Introduction

Synthetic dyes are compounds used in many industrial sectors such as the automotive, chemical, paper, plastics and especially the textile field which is a major source of water pollution and which will significantly damage the receiving waters if they are not treated [1]. The affinity between the textile and dye changes according to the chemical structure of dye and the type of fibers on which they are applied [2]. The processing and shrimp peeling industry generates every year several tons of organic waste (co-products) to landfill sites [3]. There are several techniques for the treatment of industrial effluents [4,5], adsorption is one of the most used techniques because of their simplicity and low cost [6,7].

Polymers with ion exchange and the complexing properties are recently widely used to improve the adsorption properties of mineral adsorbents. In this regard, a natural biopolymer chitosan attracts attention. The properties of the inorganic matrix of the mineral support with chitosan (silica-chitosan composite) could be improved by the valuable characteristics of a polymer [8] and especially chitosan, is a biodegradable glucosamine polymer [9] and bioresorbable, two important properties in our time where environmental protection plays an important role, chitosan can be obtained by the deacetylation of chitin [10] component of crustacean shells and especially the shrimp [11].

The objective of this research is to determine the feasibility of using silica-chitosan composite produced from nordic shrimp "Pandalus Borealis" and "Cragon-Cragon" for the removal of anionic dyes Reactive Red 23 (RR 23) and Reactive blue 19 (RB 19) in both single and binary systems of dyes.

2. Materials and methods

2.1. Analytical instruments

To characterize our product and determine the functional groups we used an infra-red spectrophotometer of type JASCO FT/IR-410 on potassium bromide pastilles KBr with 2% of Si-Cs composite. The obtained spectrum was recorded between 4000 cm^{-1} and 400 cm^{-1} . Then we used the X-ray diffraction type Bruker D8 Advance ECO to know the structure of our composite and the Scanning Electron Microscope SEM gives us an idea about the morphology surface of our adsorbent equipped with an EDXA allows a qualitative detection and the localization of the elements present in the adsorbent.

In order to determine the influencing effect of the parameters on adsorption in the single and binary systems, the measurements of the quantities adsorbed of Reactive Red 23 and Reactive Blue 19 on our composite were carried out in a analysis wavelength λ_{max} : 511 nm and λ_{max} : 592 nm, respectively, on a Spectrophotometer UV of the type JASCO V-360 with a preliminary calibration of the instrument spectrophotometer.

2.2. Materials

Chitosan with a deacetylation degree of 85% was prepared in the laboratory scale by hydrothermo-chemical extraction [1] from the northern shrimp "Pandalus Borealis" and "Cragon-Cragon". Silica with a particle size between 70-200 microns and a specific surface area of $550\text{ m}^2/\text{g}$ was purchased from the company SDS-France, acetic acid and glutaraldehyde were from Sigma-Aldrich and all other chemicals used were of analytical quality.

2.3. Methods

2.3.1. Extraction of chitosan by the hydrothermo-chemical method

The chitosan extraction by the hydrothermo-chemical method [1] was accomplished by a demineralization in acidic medium followed by simultaneous deproteination and deacetylation in basic medium according with optimal experimental conditions quoted in table 1. The solid-liquid ratio was of 1:10 (dry weight of carapace: volume of diluted solution).

Table 1: Optimal experimental conditions to extract chitosan by the hydrothermo-chemical method.

Step	Temperature (°C)	Digestive Solution	Time (h)	DD(%)
Demineralization	50	2 M HCl	2.5	-
Deproteination and deacetylation	110	12.5 M NaOH	2.0	90

2.3.2. Si-Cs composite synthesis:

To synthesize the silica-chitosan composite (Si-Cs) (Figure 1), it is first necessary to dry the silica at a temperature of 110°C for 1 hour in an oven for the activation of their surface [12], 30g of silica was immersed in 285ml of acetic acid (5%, $\text{pH}=2$) containing 2g of chitosan, then stirred the entire for 2 h, after decantation and drying oven with a temperature of 80°C , 20ml of glutaraldehyde 0.05% was added to the mixture of silica and chitosan with stirring for 2 hours and soaked in an ultrasonic bath of type Boyer Transsonic 460/H at 35 KHz for 30 min, the wet mixture was transferred into a refrigerator at 4°C for 24 hours to undergo complete crosslinking reaction [13] and washed to neutral pH and dried in an oven at 80°C and used for the adsorption studies.

2.3.3. Adsorption procedure:

The dye adsorption measurements were performed by mixing various amounts of Si-Cs composite (1mg to 100mg) for RR 23 and RB 19 in single (sin) and binary (bin) systems of dyes, in Erlenmeyer containing 30ml of a neutral pH dye solution, initial dye concentration 10mg/l with a temperature of 24°C and stirring at 150 rpm. The study of pH effect (1 to 9) on dyes adsorption in both single and binary systems was performed under a temperature of 24°C with stirring at 150 rpm using 40 mg adsorbent mass, initial dye concentration 10mg/l and

a contact time of 90 minutes, the solution was adjusted by adding a small amount of HCl or NaOH. Dye solutions were prepared using distilled water to prevent and minimize the possible interference in this study.

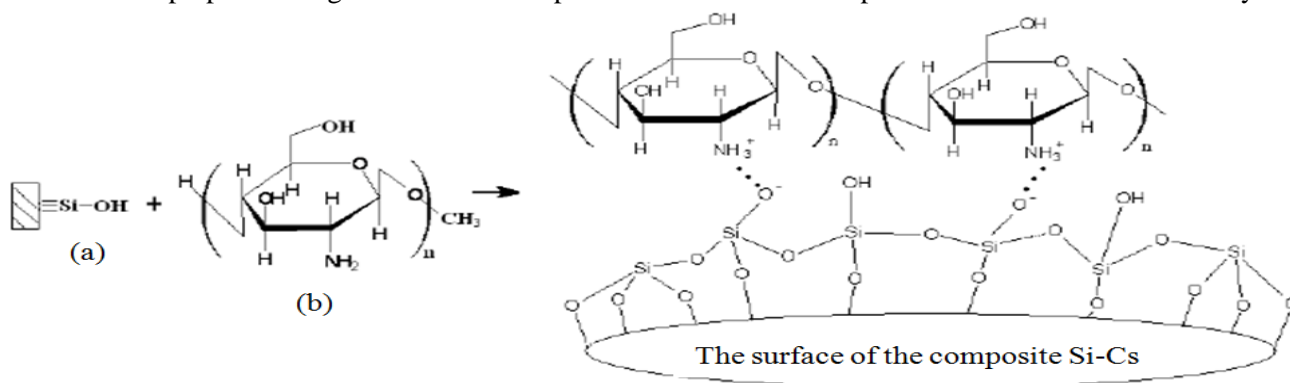


Figure 1: Chemical interaction scheme between the silica (a) and chitosan (b).

The calculation of the amount adsorbed (q_e) and the removal percentage (R%) of the two adsorbates was conducted by equations (1) and (2):

$$\text{Amount adsorbed}(q_e) = \frac{C_0 - C_e}{M} * V \quad (1)$$

$$\text{Removal}(\%) = \frac{C_0 - C_e}{C_0} * 100 \quad (2)$$

Where C_0 : initial dye concentration in solution (mg/l), C_e : final dye concentration in solution (mg/l), M : adsorbent mass (g) and V : the solution volume.

The experiments were carried out with different dyes concentrations using 40 mg of composite for RR 23 and RB 19 in single and binary systems of dyes at a neutral pH with a temperature of 24°C during 90 min under stirring at 150 rpm to reach equilibrium conditions (Table 2).

Table 2: Initial dyes concentrations used in single and binary systems of dyes.

Single system		Binary system	
C_0 (mg/l), RR23(Sin)	C_0 (mg/l), RB19(Sin)	C_0 (mg/l), RR23(Bin)	C_0 (mg/l), RB19(Bin)
10	10	5	5
25	25	12.5	12.5
50	50	25	25
60	60	30	30
75	75	37.5	37.5
100	100	50	50
125	125	62.5	62.5
150	150	75	75
175	175	87.5	87.5
200	200	100	100
225	225	112.5	112.5
250	250	125	125
275	275	137.5	137.5
300	300	150	150

Dyes concentrations in binary systems [14] were calculated using equations (3) and (4). For a binary system of components A and B, measured at λ_1 and λ_2 , respectively, to obtain optical densities of d_1 and d_2 [15,16]:

$$C_A = (k_{B2}d_1 - k_{B1}d_2) / (k_{A1}k_{B2} - k_{A2}k_{B1}) \quad (3)$$

$$C_B = (k_{A1}d_2 - k_{A2}d_1) / (k_{A1}k_{B2} - k_{A2}k_{B1}) \quad (4)$$

Where C_A and C_B are the concentrations of components A and B in binary systems, respectively. k_{A1} , k_{B1} , k_{A2} , and k_{B2} are the calibration constants for components A and B at the two wavelengths of λ_1 and λ_2 , respectively.

Absorbance changes were determined in various time intervals (10, 20, 30, 60, 120, 180, 240 and 300min) during the adsorption process to determine adsorption kinetics under following conditions: a temperature of 24°C, adsorbent mass 40 mg, initial dye concentration 60 mg/l, pH~7 and stirring at 150 rpm. To study the

effect of the temperature on adsorption one used an adsorbent mass of 40 mg with an initial dye concentration of 60 mg/l under continuous stirring at 150 rpm during 90min for various temperatures (25°C, 45°C, 65°C and 85°C). Then, samples were centrifuged by P.SELECTA Mixtasel centrifugal machine, and dyes concentrations were given.

Results were verified by the adsorption isotherms (Freundlich, Langmuir, Temkin and Dubinin-Radushkevich) and kinetics (pseudo-first-order, pseudo-second-order, the intraparticle diffusion model and the Elovich model) and thermodynamic parameters were calculated to describe the adsorption.

3. Results and discussion

3.1. Characterization of Si-Cs composite

For determining the immobilization of chitosan on the silica surface. FT-IR spectroscopy was used to characterize the initial chitosan (Cs), silica (Si) and Silica-Chitosan composite (Si-Cs), figure 2 shows infrared spectra of Cs, Si and composite Si-Cs. The Si-Cs composite bands 3439cm^{-1} , 1657cm^{-1} , 1559cm^{-1} , 1084cm^{-1} and 467cm^{-1} are assigned to stretching vibration of the surface hydroxyl, the band of azomethine formed after treatment with glutaraldehyde, vibration of deformation of the amino group protonated $-\text{NH}_3^+$, the stretching vibration of Si-O and twisting vibration of Si-O-Si, respectively [17]. The major bands for chitosan can be assigned as follows: 3436cm^{-1} ($-\text{OH}$ and $-\text{NH}_2$ stretching vibrations), 2930cm^{-1} ($-\text{CH}$ stretching vibration in $-\text{CH}$ and $-\text{CH}_2$), 1659cm^{-1} ($-\text{NH}_2$ bending vibration), 1379cm^{-1} ($-\text{CH}$ symmetric bending vibrations in $-\text{CHOH}$), 1076cm^{-1} and 1026cm^{-1} ($-\text{CO}$ stretching vibration in $-\text{CONH}$) [18,19].

Figure 3 present the X-ray power diffraction patterns of chitosan, silica and composite Si-Cs. Chitosan shows characteristic peaks in $2\theta=9.2^\circ$; 12.5° ; 19.8° ; 26.03° and 39.4° [20]. Silica showed characteristic peaks in $2\theta=10.0^\circ$ and 22.0° [21]. These peaks correspond to a crystalline structure of chitosan and silica, respectively. XRD spectra of Si-CS composite are more or less amorphous in nature with small crystalline area between $2\theta=9^\circ$ and 26° . The decrease in the crystallinity may be due to introduction of bulky chitosan polymeric chain, which demonstrates that the conjugation of silica and chitosan suppressed the crystallization to some extent. It suggests that silica and chitosan polymeric chain were mixed well at a molecular level.

A SEM images of chitosan (A), silica (B) and Si-Cs composite (C) are shown in figure 4, the SEM micrograph of chitosan (A) indicates a smooth morphology, on the other hand on the silica level (B) one observes the presence of a more or less porous structure, The SEM micrograph of the Si-Cs composite indicates many of surface pores are not smooth and porous in structure with the presence of chitosan attached to the surface which shows that the chitosan immobilized well on the silica surface.

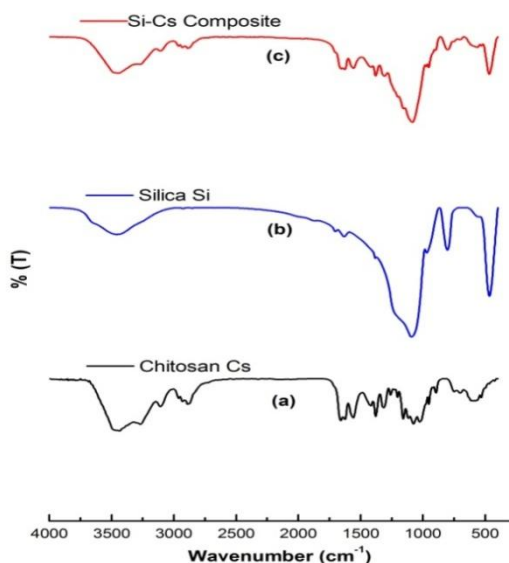


Figure 2: FT-IR spectra of the Cs (a), Si (b) and Si-Cs (c).

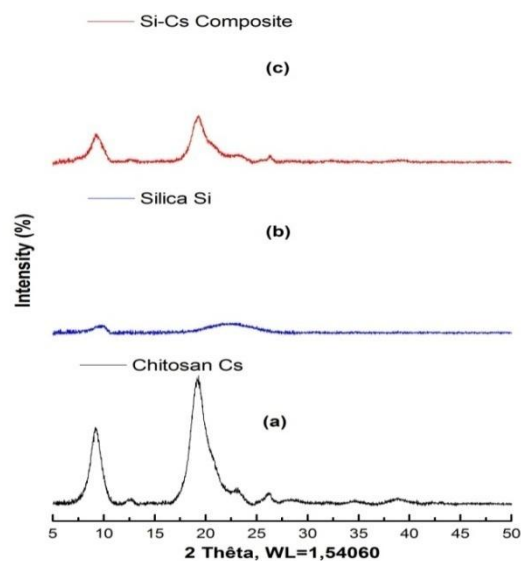


Figure 3: XRD spectra of the Cs (a), Si (b) and Si-Cs (c).

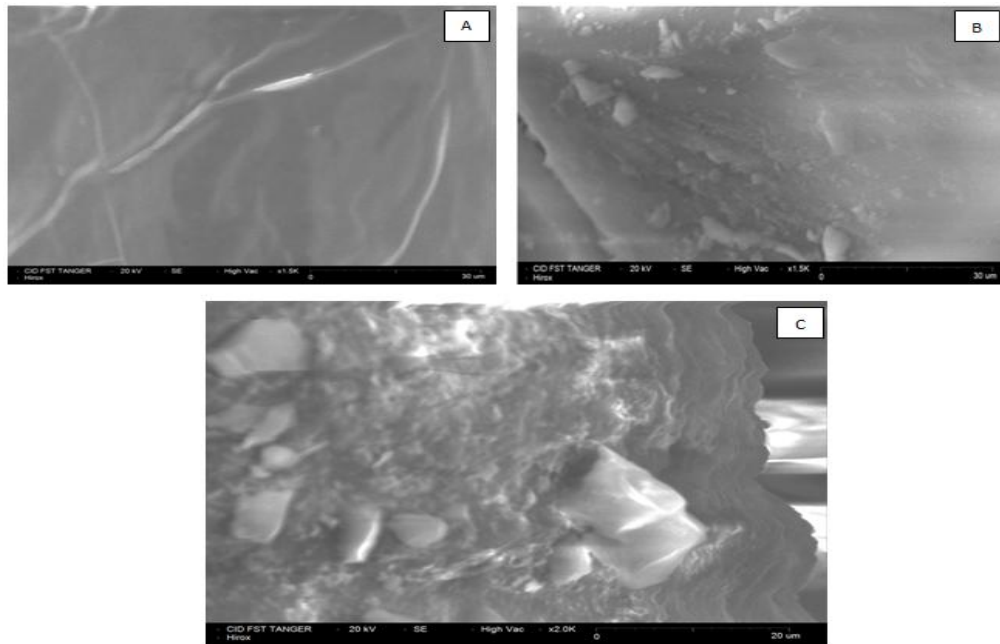


Figure 4: SEM of chitosan (A), silica (B) and Si-Cs composite (C).

The EDXA spectra of the Si-Cs composite also confirm the presence of C, N, O and Si in the composite and the quantitative elemental composition of chitosan (A), silica (B) and Si-Cs composite (C) are listed in the figure 5.

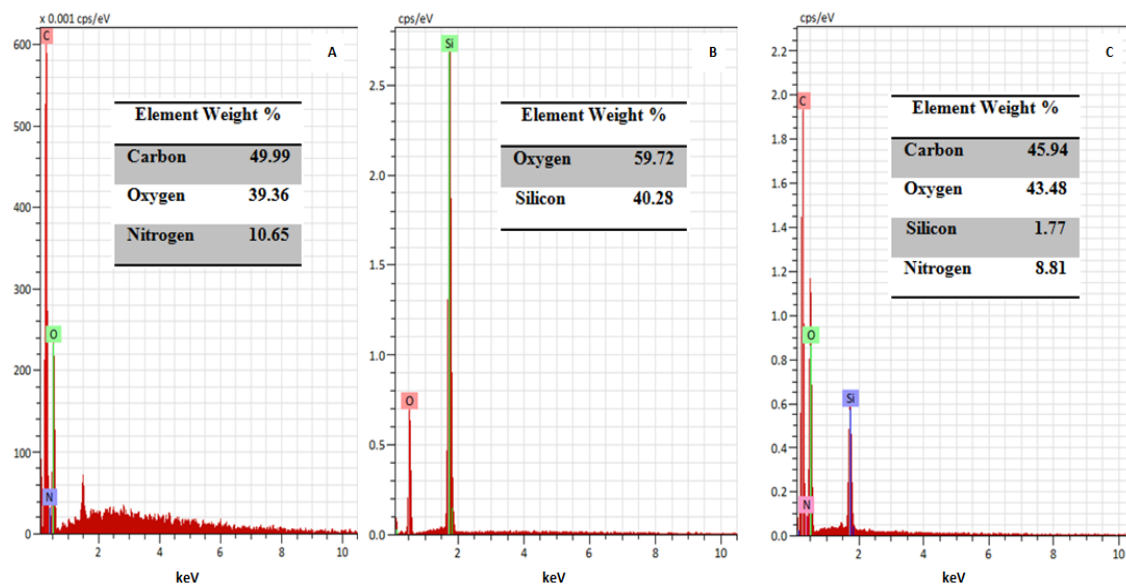


Figure 5: EDXA spectra of chitosan (A), Silica (B) and Si-Cs composite (C).

3.2. Operational parameters effect on the removal of dyes

3.2.1. Effect of adsorbent dose

The influence study of Si-Cs composite amount on the adsorption of dyes RR 23 and RB19 in single (sin) and binary (bin) systems was carried out in Erlenmeyers containing 30 ml of dye solution with neutral pH at a temperature of 24°C under stirring at 150 rpm with an initial dye concentration 10mg/l during 90 min. Various quantities of composite (1mg to 100mg) for RR 23 and RB 19 were applied. After balance, the samples were centrifuged and the concentration in the supernatant dye solution was analyzed.

Figure 6 shows the effect of adsorbent amount on the elimination of dyes starting from the single and binary systems of dyes. Dyes elimination percentage (R%) increases with the increase in the adsorbent amount until some limit then it reaches a constant value, the optimal adsorbent amounts for RR23 and RB19 elimination in single and binary systems are presented in table 3.

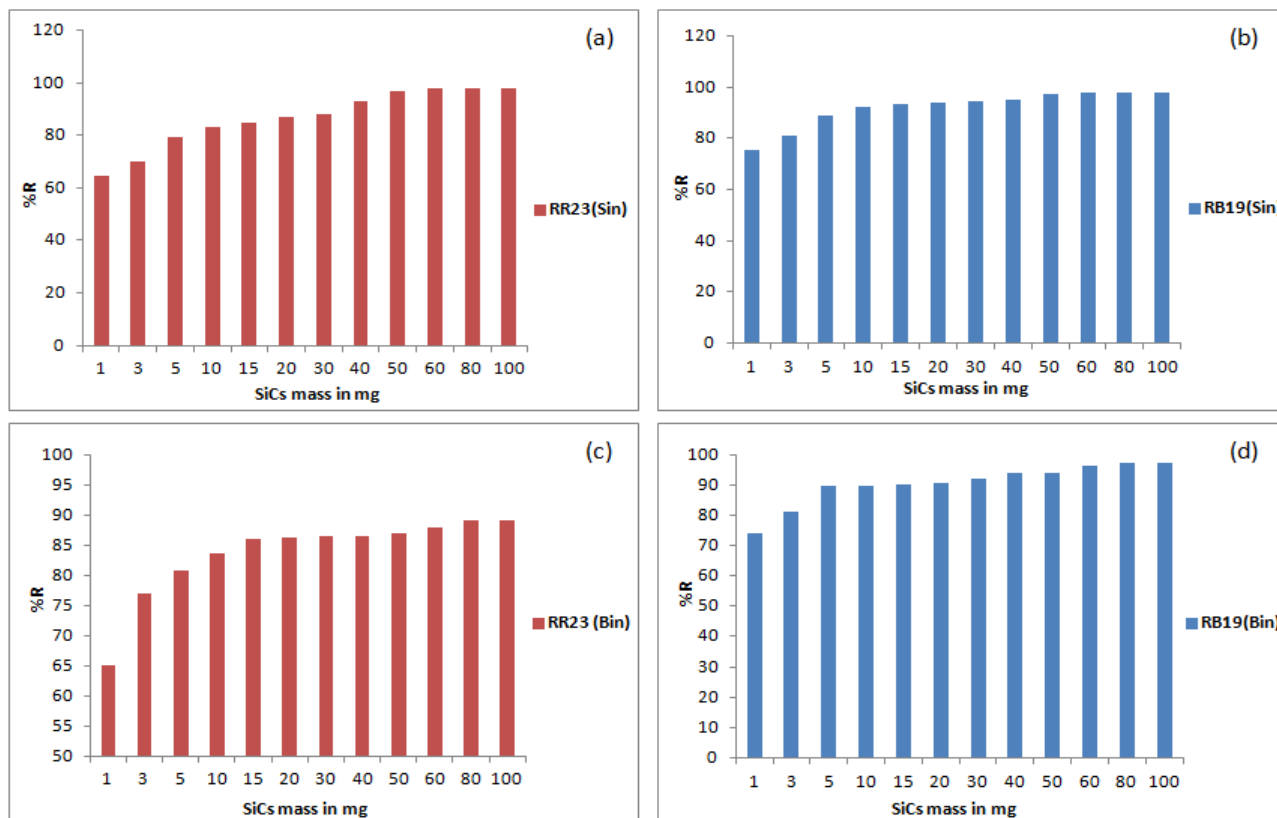


Figure 6: Effect of adsorbent amount (Si-Cs) on the adsorption of dyes (a) RR23 (Sin), (b) RB19 (Sin), (c) RR23 (Bin) and (d) RB19 (Bin). (Time=90min; Temperature=24°C; Initial dye concentration=10mg/l; Stirring=150 rpm and pH~7)

Table 3: Optimal adsorbent amount for RR 23 and RB 19 elimination in single and binary systems of dyes.

System		Optimal adsorbent amount in mg	R%
Single	RR23	50	97
	RB19	50	97
Binary	RR23	60	89
	RB19	60	97

The increase in adsorption with the adsorbent amount can be allotted to the increase in the adsorbent surface and the availability of several sites of adsorption. However, if the adsorption capacity was expressed by mg adsorbed per gram of material, the capacity decreases with increasing the adsorbent quantity. That can be attributed to the overlapping or the aggregation of the adsorption sites involving a reduction in the entire adsorbent surface available for the dyes and increased the length of the diffusion path [22]. If we compare these results with our previous work [1], we can notice that we need a lower adsorbent amount for reaching a higher removal percentage with respect to chitosan alone [1].

3.2.2. Effect of pH

At a low pH more protons are available to protonate the amine groups of chitosan to form NH_3^+ groups on the composite surface, thus increasing the electrostatic attraction between the negatively charged anions dyes and positively charged adsorption sites, causing an increase of dyes adsorption (figure 7). Si-Cs composite is composed of various functional groups such as amine groups of chitosan, hydroxyl and carbonyl groups can also be affected by the pH of the solution.

It can be seen that the pH of the aqueous solution plays an important role in the anionic dyes adsorption on Si-Cs composite. Chitosan attached to the composite surface contains amine groups, $-\text{NH}_2$, which is easily protonated to form $-\text{NH}_3^+$, in acidic solutions.

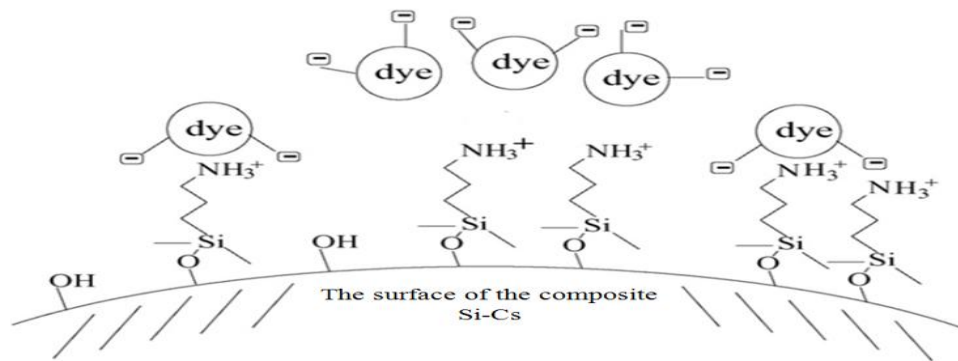


Figure 7: Schematic representation of anionic dyes interaction with Si-Cs composite in an acidic solution.

The effect of pH on the adsorption of RR 23 and RB 19 in single and binary systems of dyes on the Si-Cs composite is shown in figure 8. The maximum dye adsorption occurred at pH 1.

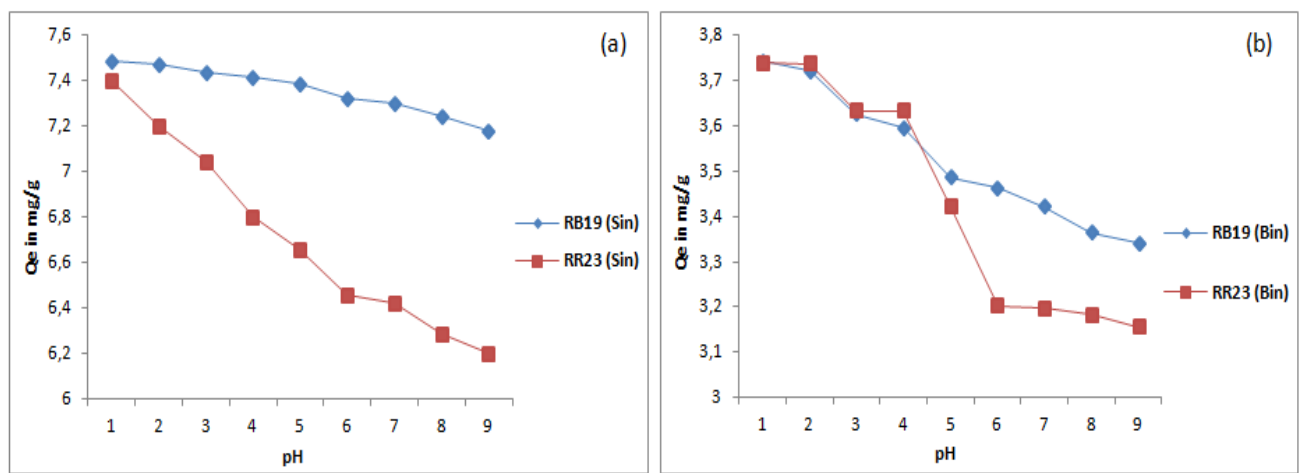


Figure 8: The effect of pH on the adsorption of RR 23 and RB 19 on the Si-Cs composite in single (a) and binary (b) systems of dyes. (Time=90 min; Temperature=24°C, Initial dye concentration =10mg/l; Adsorbent mass=40mg; Stirring=150 rpm).

Dyes RR 23 and RB 19 are dissociated to polar groups ($R-SO_3^-$). Therefore, at different pH values, electrostatic attractions, organic properties and structure of dyes molecules and composite could play a very important role in dyes adsorption on the Si-Cs composite.

At pH 1, a significantly high electrostatic attraction between the positively charged adsorbent surface and negatively charged anionic dyes because of the ionization of adsorbent functional groups. When the pH of the system increases, the numbers of negatively charged sites are increased. A negatively charged site on the adsorbent does not promote the adsorption of anionic dyes due to the electrostatic repulsion. In addition, adsorption of RR 23 and RB 19 is less in single and binary systems of dyes at alkaline pH is due to the presence of OH^- ions in excess causing the destabilization of anionic dyes and compete with them for adsorption sites.

3.2.3. Effect of initial dye concentration

Effect of initial dye concentration RR 23 and RB 19 in both single and binary systems were studied. Si-Cs composite (40mg for RR 23 and RB 19 in both single and binary systems of dyes) were added to 30ml of RR23 and RB19 in single and binary systems at different dyes concentrations (10mg/l, 25mg/l, 50mg/l to 300mg/l) table 2. These experiments were performed at a neutral pH with a temperature of 24°C for 90 min under stirring at 150 rpm. For both single and binary systems of dyes the adsorption capacity increases with increasing the initial dye concentration to reach a bearing which represents the state of equilibrium as shown in figure 9, this is due to the increase in the driving force of concentration gradient with the increase in the initial dye concentration. At a fixed adsorbent dosage, the amount adsorbed increased with increasing concentration of solution, but the adsorption percentage decreased. In other words, the residual concentration of dye molecules will be higher for higher initial dye concentrations. In the case of lower concentrations, the ratio of initial

number of dye molecules to the available adsorption sites is low and subsequently the fractional adsorption becomes independent of initial concentration [23-25].

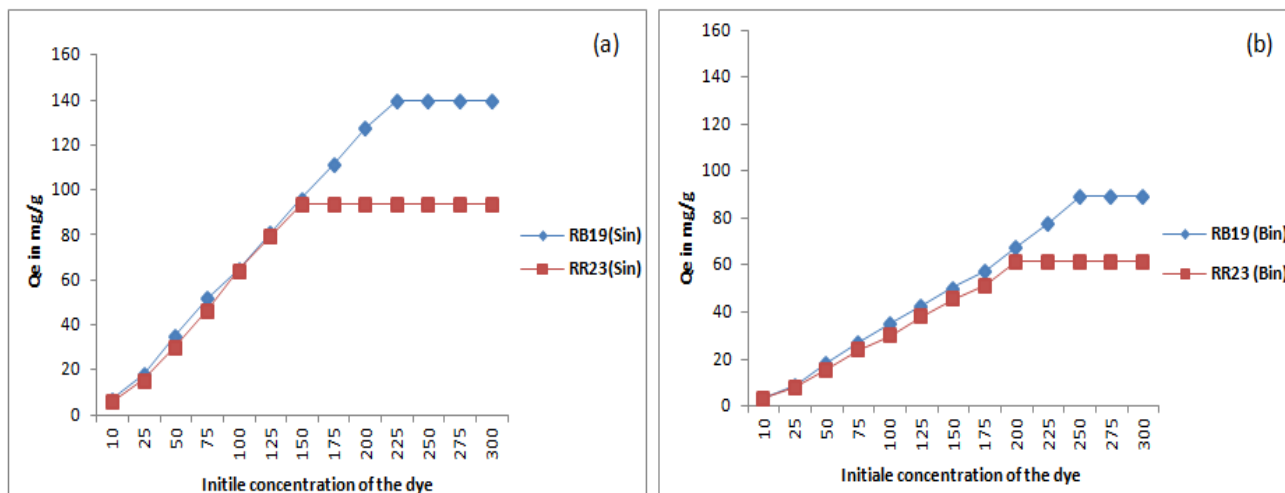


Figure 9: Effect of initial dye concentration on the adsorption of RR 23 and RB 19 in single (a) and binary (b) systems. (Time=90min; Temperature=24°C; Adsorbent mass=40mg; stirring=150 rpm and pH~7)

From figure 9 we can see that the optimal dyes concentrations are obtained only from the bearing, they are equal to 125mg/l and 200mg/l for RR 23 and RB 19 in the single system of dye, respectively, and in the binary system the optimal dyes concentrations are 175mg/l and 225mg/l for RR 23 and RB 19, respectively, indicating that the binary system required higher initial dye concentration than the single system to reach the adsorption equilibrium state.

3.2.4. Effect of contact time

The influence study of contact time on the adsorption is critical to determine the contact time relating to the adsorption equilibrium or saturation state of the support with the adsorbate. Figure 10 shows the evolution of retention performance of RR 23 and RB19 in single and binary systems of dyes based on the contact time of liquid/solid. The obtained results showed that the efficiency increases with increasing of contact time to reach equilibrium after 180 minutes for the RR 23 and RB 19 in both single and binary systems of dyes.

3.3. Adsorption isotherm models in single and binary systems of dyes

Several isotherm models were used in literature to describe the experimental data of adsorption isotherms. In order to optimize the design of an adsorption system for removing dyes from solutions, it is important to establish the most suitable correlation for the equilibrium curve. The Langmuir model is the most commonly used model [26], is given by the equation:

$$q_e = \frac{Q_0 K_L C_e}{1 + K_L C_e} \quad (5)$$

Where q_e , C_e , Q_0 and K_L are the amount of solute adsorbed at equilibrium (mg/g), the concentration of adsorbate at equilibrium (mg/l), maximum adsorption capacity (mg/g) and Langmuir constant (L/mg), respectively. The essential characteristics of Langmuir isotherm can be expressed by a dimensionless constant called equilibrium parameter R_L , which is defined by the following equation [27]:

$$R_L = 1/(1+K_L C_e) \quad (6)$$

R_L indicates that the adsorption is effective when it is between 0 and 1, it is equal to zero when it is greater than 1. In this work, an expanded Langmuir model was used to fit the experimental data [28].

$$q_{e,i} = \frac{(Q_0 K_{L,i} C_{e,i})}{(1 + \sum K_{L,i} C_{e,i})} \quad (7)$$

Where $K_{L,i}$ is the adsorption equilibrium constant of dye I in mixed dye system. In dye adsorption from binary systems, the amounts of dye adsorbed were expressed as:

$$q_{e,1} = \frac{(K_{L,1} Q_{0,1} C_{e,1})}{(1 + K_{L,1} C_{e,1} + K_{L,2} C_{e,2})} \quad (8)$$

$$q_{e,2} = \frac{(K_{L,2} Q_{0,2} C_{e,2})}{(1 + K_{L,1} C_{e,1} + K_{L,2} C_{e,2})} \quad (9)$$

1 ($R_L > 1$); $R_L = 0$, the adsorption is irreversible and $R_L = 1$, the representation of the isotherm is linear.

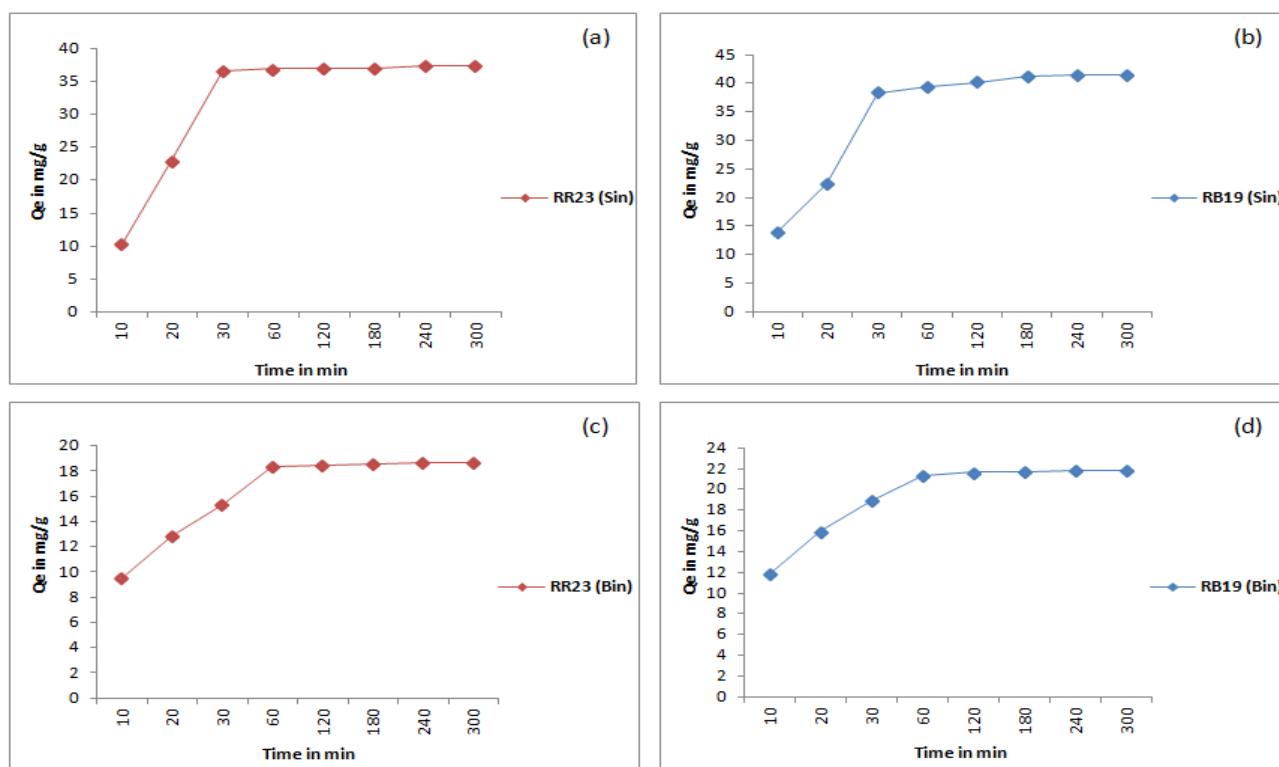


Figure 10: Effect of contact time on the adsorption of dyes on the Si-Cs composite (a) RR23 (Sin), (b) RB19 (Sin), (c) RR23 (Bin) and (d) RB19 (Bin). (Temperature=24°C; Adsorbent mass=40mg; Initial dye concentration=60mg/l; Stirring=150rpm and pH~7)

According to equations (8) and (9), we have:

$$\frac{(K_{L,2}C_{e,2})}{(K_{L,1}C_{e,1})} = \frac{(Q_{0,1}q_{e,2})}{(q_{e,1}Q_{0,2})} \quad (10)$$

After rearrangement, a linear form of the expanded Langmuir model in binary dye system was obtained [16].

$$\left(\frac{C_{e,1}}{q_{e,1}}\right) = \left(\frac{1}{K_{L,1}Q_{0,1}}\right) + \left(\frac{C_{e,1}}{Q_{0,1}}\right) + \left(\frac{q_{e,2}C_{e,1}}{q_{e,1}Q_{0,2}}\right) \quad (11)$$

According to equation (11), the values of $C_{e,1}/q_{e,1}$ had linear correlation with $C_{e,1}$ and $C_{e,1} q_{e,2}/q_{e,1}Q_{0,2}$ if the adsorption obeyed the expanded Langmuir model. By using equation (11) as the fitting model, the isotherm parameters of an individual dye in the binary dye solution were estimated.

The Freundlich model is based on the hypothesis of energy surface heterogeneity, the empirical equation of this model is presented in the form [6]:

$$\ln Q_e = \ln K_f + \ln C_e / n_f \quad (12)$$

Where K_f and n_f are the Freundlich characteristic constants, with K_f represents the relative adsorption capacity of the adsorbent and n_f the dependence degree of adsorption on the adsorbate equilibrium concentration.

The model of Temkin assumes that the liquid/solid interactions are not negligible and that the adsorption energy of the molecules is reduced with the coverage ratio of the surface. The linear transform of Temkin isotherm is presented in the form [16]:

$$q_e = B_1 \ln K_T + B_1 \ln C_e \quad (13)$$

Where

$$B_1 = RT / b$$

K_T is the Temkin isotherm equilibrium binding constant (1/g), B_1 is the constant related to heat of sorption (J/mol), b represents the Temkin isotherm constant, R and T are the universal gas constant (8.314 J/mol/K) and the absolute temperature (K), respectively.

Tempkin isotherm contains a factor that explicitly takes into the account adsorbing species adsorbent interactions. This isotherm assumes that the adsorption heat of all the layer molecules decreases linearly with coverage due to adsorbent–adsorbate interactions, and that the adsorption is characterized by a uniform distribution of binding energies, up to some maximum binding energy.

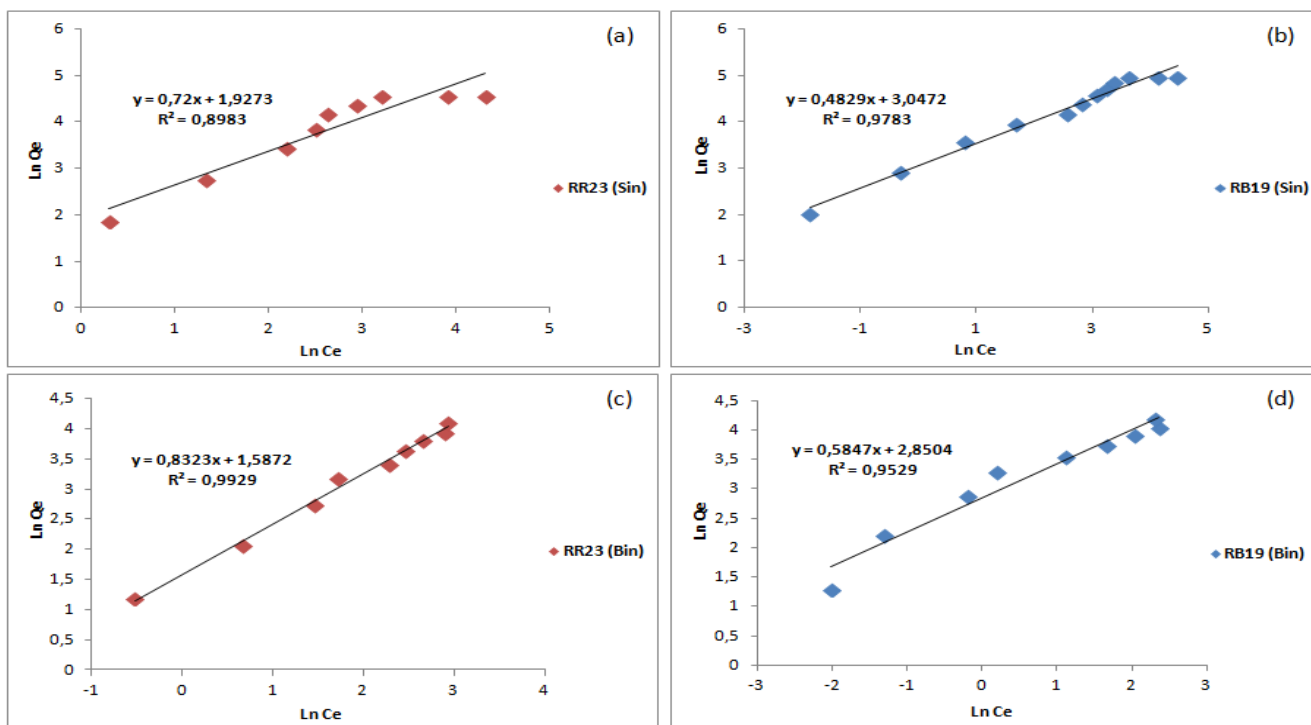


Figure 11: Freundlich isotherm model for the adsorption of RR23 and RB19 on Si-Cs composite in single and binary systems of dyes (a) RR23 (Sin), (b) RB19 (Sin), (c) RR23 (Bin) and (d) RB19 (Bin). (Time=90min; Temperature=24°C; Adsorbent mass=40mg; Stirring=150rpm and pH~7)

Dubinin–Radushkevich isotherm [29] is generally applied to express the adsorption mechanism with a Gaussian energy distribution onto a heterogeneous surface. The model has often successfully fitted high solute activities and the intermediate range of concentrations data well.

$$q_e = (q_s) \exp(-K_{ad} \varepsilon^2)$$

$$\ln q_e = \ln(q_s) - (K_{ad} \varepsilon^2) \quad (14)$$

Where q_e =amount of adsorbate in the adsorbent at equilibrium (mg/g); q_s = theoretical isotherm saturation capacity (mg/g); K_{ad} =Dubinin–Radushkevich isotherm constant (mol^2/kJ^2) and ε =Dubinin–Radushkevich isotherm constant. The approach was usually applied to distinguish the physical and chemical adsorption of metal ions with its mean free energy, E per molecule of adsorbate (for removing a molecule from its location in the sorption space to the infinity) can be computed by the relationship [30,31]:

$$E = \left[\frac{1}{\sqrt{2B_{DR}}} \right] \quad (15)$$

Where B_{DR} is denoted as the isotherm constant. The parameter ε can be calculated as:

$$\varepsilon = RT \ln \left[1 + \frac{1}{C_e} \right] \quad (16)$$

Where R , T and C_e represent the gas constant (8.314J/mol. K), absolute temperature (K) and adsorbate equilibrium concentration (mg/l), respectively. One of the unique features of the Dubinin-Radushkevich (DRK) isotherm model lies on the fact that it is temperature-dependent, which when adsorption data at different temperatures are plotted as a function of logarithm of amount adsorbed ($\ln q_e$) versus ε^2 the square of potential energy, all suitable data will lie on the same curve, named as the characteristic curve. To investigate the applicability of Langmuir, Freundlich, Temkin and Dubinin-Radushkevich isotherms for the adsorption of dye on Si-Cs composite in single and binary systems of dyes, linear plots of C_e/Q_e against C_e , $\ln Q_e$ versus $\ln C_e$ (Figure 11), Q_e versus $\ln C_e$ and $\ln Q_e$ against ε^2 are plotted respectively and the values of Q_0 , K_L , R_L , K_f , n_f , K_T , B_1 , b , Q_s , K_{ad} , E and R^2 (correlation coefficient values of all isotherms models) are shown in table 4.

The values of the correlation coefficients (R^2) show that the dyes removal isotherm in both single and binary system by using Si-Cs composite does not follow the Lungmuir, Temkin and Dubinin-Radushkevich isotherms (Table 4). The correlation coefficient calculated (R^2) for the Freundlich isotherm model (Figure 11) shows that

the dye removal isotherm can be approximate like the model of Freundlich (Table 4-Figure 11), This means that there is a heterogeneity of surface energy with a nonuniform distribution of the adsorption heat on surface and the adsorption is not limited to the formation of monolayer.

Table 4: Isotherm constants for dyes adsorption RR23 and RB19 on Si-Cs composite in single and binary systems. (Time=90min; Temperature=24°C; Adsorbent mass=40mg; Stirring=150rpm and pH ~ 7)

System	Lungmuir Isotherm				Freundlich Isotherm			Temkin Isotherm			Dubinin-Radushkevich Isotherm				
	Q ₀	K _L	R _L	R ²	K _f	n _f	R ²	K _T	B ₁	b	R ²	Q _s	K _{ad}	E	R ²
Single	RR 23														
	128.2	0.050	0.209-0.936	0.916	6.870	1.388	0.898	0.692	26.396	93.861	0.878	62.433	0.002	14.202	0.728
Binary	RB 19														
	156.25	0.104	0.097-0.984	0.970	21.056	2.070	0.978	3.310	24.119	102.722	0.884	84.318	0.001	23.416	0.676
Binary	RR 23														
	151.51	0.299	0.149-0.849	0.698	4.890	1.201	0.992	0.093	15.891	155.910	0.846	32.168	0.003	11.708	0.698
Binary	RB 19														
	73.52	0.387	0.205-0.951	0.956	17.294	1.710	0.952	1.931	13.286	186.479	0.940	43.341	0.003	12.868	0.902

3.4. Adsorption kinetic models in single and binary systems of dyes

To develop a fast and efficient model, multiple kinetic models can be used to express the adsorption mechanism in a solution. To review the control mechanisms of the adsorption process, such as chemical reactions, controlling the diffusion and mass transfer, several kinetic models are used to test the experimental data. The pseudo first order model is generally represented as follows [32]:

$$\frac{dq_t}{dt} = k_1(q_e - q_t) \quad (17)$$

Where q_e : the dye amount adsorbed at equilibrium (mg/g), q_t : the dye amount adsorbed at time t (mg/g) and k_1 : the equilibrium rate constant of pseudo-first-order kinetics (1/min) and t : contact time (min).

After integration by applying conditions, $q_t=0$ at $t=0$, then equation (17) becomes:

$$q_t = q_e (1 - e^{-k_1 t}) \quad (18)$$

The linearization of the previous equation gives [33]:

$$\ln(q_e - q_t) = \ln q_e - k_1 t \quad (19)$$

One traces $\ln(q_e - q_t) = f(t)$, one obtains a line which gives k_1 and q_e . This model can describe the phenomena occurring during the first minutes of the adsorption process.

The pseudo-second-order model is given by the following expression [33,34]:

$$\frac{dq_t}{dt} = k_2(q_e - q_t)^2 \quad (20)$$

Where k_2 : the reaction speed constant of second order adsorption in (g/mg/min), q_e : the dye amount adsorbed at equilibrium in (mg/g), q_t : the dye amount adsorbed at time t (mg/g), t : contact time in (min). After integration one obtains:

$$q_t = \left(\frac{k_2 q_e^2 t}{k_2 q_e t + 1} \right) \quad (21)$$

The linearization of the previous equation gives [33,34]:

$$\frac{t}{q_t} = \frac{1}{k_2 q_e^2} + \frac{1}{q_e} t \quad (22)$$

One traces $t/q_t = f(t)$, one obtains a line which gives k_2 and q_e . Contrary to the model of first order, the model of pseudo-second-order is applicable to a broader time interval (generally the entire adsorption process).

To study the possibility of dyes molecules transport by the adsorbent particles, one uses the equation of Weber and Morris which represents the intraparticle diffusion model [35,36]:

$$q_t = k_i t^{1/2} + c \quad (23)$$

q_t : the amount adsorbed at time t (mg/g), C : the intersection of the line with the Y-axis, the value of C gives an idea about the thickness of the boundary layer, as more the ordinate at the origin value is greater, the effect of the boundary layer is more important, K_i : the intraparticle diffusion constant (mg/g.min^{1/2}). If one traces q_t according to $t^{1/2}$ one can determine the constant K_i and the thickness of boundary layer C .

The Elovich model can be expressed by the equation [33,37]:

$$\frac{dq_t}{dt} = \alpha \exp(-\beta q_t) \quad (24)$$

Where α : the initial adsorption speed (mg/g.min) and β : the desorption constant (g/mg). To simplify the Elovich equation it was supposed that $\alpha \beta t \gg 1$ and that $q_t=0$ with $t=0$, therefore one obtains:

$$q_t = \frac{1}{\beta} \ln(\alpha\beta) + \frac{1}{\beta} \ln t \quad (25)$$

One traces $q_t=f(\ln t)$ to determine the values of α and β .

To understand the applicability of pseudo-first-order, pseudo-second-order, intraparticle diffusion and Elovich kinetics models, linear plots of $\ln(q_e - q_t)$ versus contact time (t), t/q_t versus contact time (t) (Figure 12), q_t against $t^{1/2}$ and q_t versus $\ln(t)$ are plotted and the values of K_1 , K_2 , K_i , C , β , α , R^2 , $q_{e,exp}$, $q_{e,cal}$ (R^2 correlation coefficient values and $q_{e,exp}$, $q_{e,cal}$ for all kinetics models) are shown in table 5.

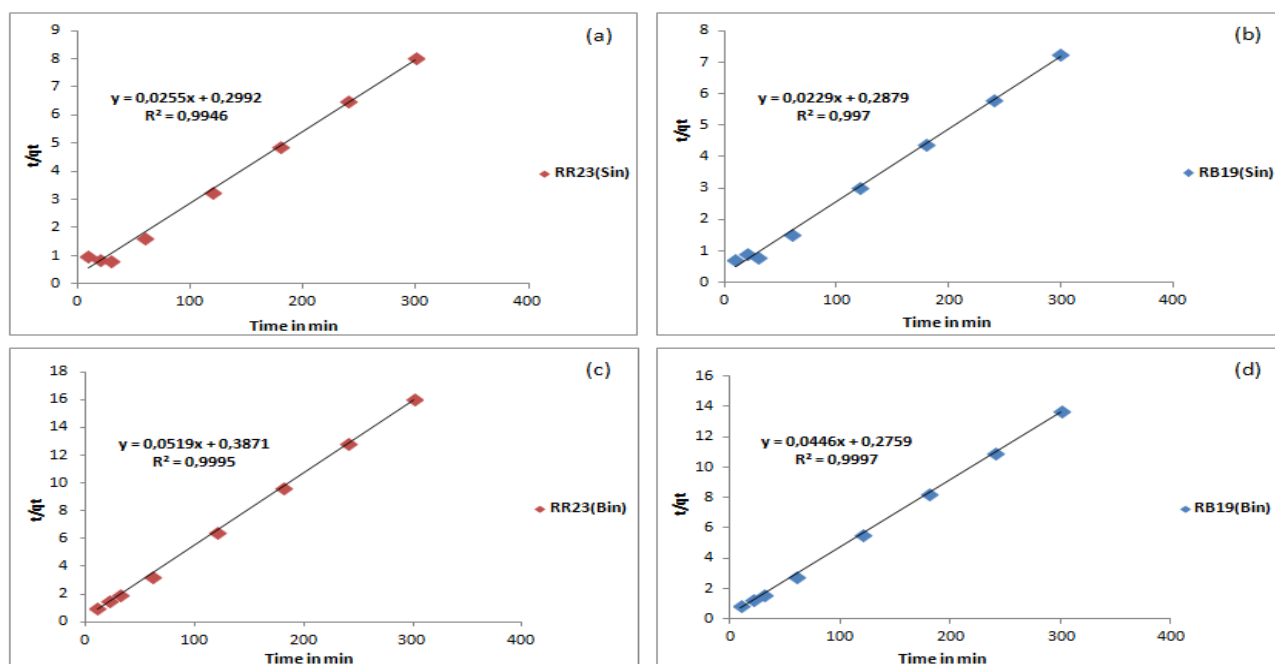


Figure 12: The pseudo-second-order kinetic model of dyes adsorption on the Si-Cs composite (a) RR23 (Sin), (b) RB19 (Sin), (c) RR23 (Bin) and (d) RB19 (Bin). (Temperature=24°C; Adsorbent mass=40mg; Initial dye concentration=60 mg/l; Stirring=150 rpm and pH~7)

Table 5: Adsorption kinetics constants of RR23 and RB19 on the Si-Cs composite in single and binary systems of dyes. (Temperature=24°C; Adsorbent mass=40mg; Initial dye concentration=60 mg/l; Stirring=150 rpm and pH~7)

System	$(q_e)_{Exp}$	Pseudo-first-order			Pseudo-second-order			Intraparticle diffusion			Elovich model		
		$(q_e)_{Cal.}$	k_1	R^2	$(q_e)_{Cal.}$	k_2	R^2	K_i	C	R^2	α	β	R^2
Single	RR23												
	37	56.610	0.111	0.813	39.215	0.002	0.994	1.281	19.401	0.466	13.175	0.155	0.645
Binary	RB19												
	41	18.602	0.029	0.733	43.668	0.001	0.997	1.497	20.164	0.567	12.417	0.137	0.735
Binary	RR23												
	18.682	6.378	0.025	0.825	19.267	0.006	0.999	0.530	11.135	0.666	22.477	0.393	0.836
Binary	RB19												
	21.880	6.684	0.025	0.849	22.421	0.007	0.999	0.555	13.999	0.638	54.460	0.373	0.814

The best model established for the adsorption kinetics study is selected according to the correlation factor. From the results of Figure 12 and Table 5, we find that the model that presents the highest correlation factor is the pseudo-second-order model, we can deduce that the pseudo-second-order model is the one that best described the adsorption process of the two dyes RR23 and RB19 on the Si-Cs composite in both single and binary systems, we also see that the adsorbed amounts calculated (q_e)_{Cal} by this model are closer to the quantities adsorbed experimentally (q_e)_{Exp}.

3.5. Effect of temperature and thermodynamic parameters

The temperature has a major effect on the adsorption process. Increasing the temperature of the solution promotes molecules diffusion across the outer boundary and internal pores of the adsorbent layer particles, perhaps because of the decrease in viscosity. These affect the adsorption capacity. The curves in Figure 13 reflect the thermal agitation effect of the adsorbed amounts of RR 23 and RB 19 in both single and binary systems of dyes. The results indicate that the temperature disadvantage retention of RR 23 and RB 19 in both single and binary systems studied [38].

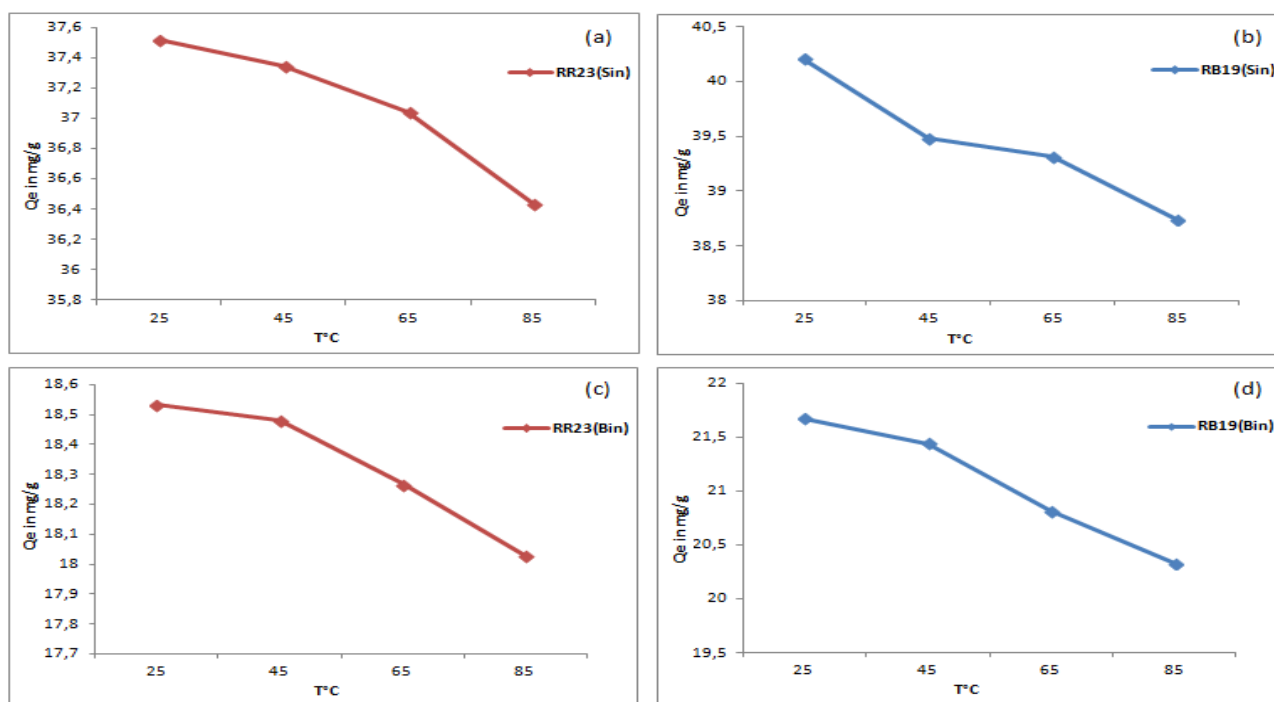


Figure 13: Effect of temperature on dyes adsorption on Si-Cs composite in single and binary systems of dyes (a) RR23 (Sin), (b) RB19 (Sin), (c) RR23 (Bin) and (d) RB19 (bin). (Adsorbent mass =40 mg; Initial dye concentration =60mg/l; Time=90min; Stirring=150rpm and pH~7)

The thermodynamic parameters are required in determining the nature and type of matter transfer phenomena at the solid-liquid interface, to calculate the thermodynamic parameters: the free energy ΔG° , the enthalpy ΔH° and the entropy ΔS° , the following equations are used [6,39]:

$$\ln K_d = \Delta S^\circ/R - \Delta H^\circ/RT \quad (26)$$

Or:

ΔH° : enthalpy (kJ/mol), ΔS° : entropy (J/mol.K), T: temperature in Kelvin, R: the gas constant (R=8.314 J/mol.K) and K_d is the distribution coefficient is calculated by the equation (27):

$$K_d = (C_0 - C_e) * V / (C_e * m) \quad (27)$$

Where C_0 : initial dye concentration in solution (mg/l), C_e : the equilibrium concentration (mg/l), m: adsorbent mass (g), V: the solution volume and Q_e : the quantity adsorbed per unit adsorbent mass at equilibrium (mg/g).

The values of the free energy ΔG° at different temperatures are calculated by the equation (28):

$$\Delta G^\circ = -RT \ln K_d \quad (28)$$

The values of ΔH° and ΔS° can be obtained from the right (Figure 14) showing the variation of $\ln K_d$ versus $1/T$, where $\Delta H^\circ/R$ is the slope and $\Delta S^\circ/R$ is the origin. The thermodynamic parameters are summarized in table 6.

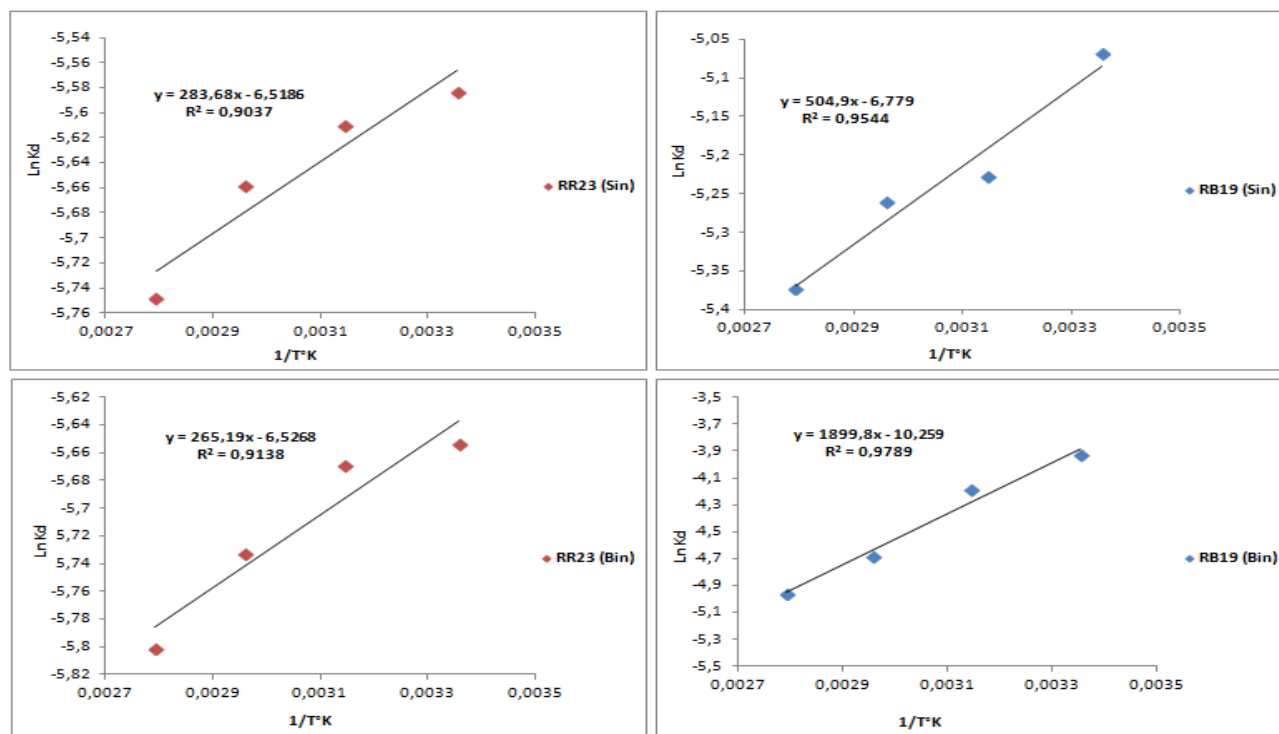


Figure 14: Representation of $\ln K_d$ versus $1/T$ to determine the thermodynamic parameters of dyes adsorption on Si-Cs composite in single and binary systems RR23 (Sin), RB19 (Sin), RR23 (Bin) and RB19 (Bin). (Adsorbent mass =40 mg; Initial dye concentration =60 mg/l; Time=90min; Stirring=150rpm and pH~7)

Table 6: Thermodynamic parameters ΔG° , ΔH° and ΔS° relating to the adsorption of RR23 and RB19 in both single and binary systems of dyes. (Adsorbent mass =40 mg; Initial dye concentration=60 mg/l; Time=90min; Stirring=150rpm and pH~7)

System	ΔH° (kJ/mol)	ΔS° (J/mol.K)	ΔG° (kJ/mol)				
			298 °K	318 °K	338 °K	358 °K	
Single	RR23	-2.358	-54.195	13.833	14.831	15.898	17.108
	RB19	-4.197	-56.360	12.559	13.820	14.784	15.989
Binary	RR23	-2.204	-54.263	14.008	14.989	16.110	17.267
	RB19	-15.794	-85.293	9.741	11.071	13.155	14.758

Table 6 gives the values of standard free enthalpy ΔG° (the free energy), standard enthalpy ΔH° and standard entropy ΔS° . According to these results, it is observed that the standard enthalpy ΔH° is negative which indicates that the adsorption process is exothermic [2] for single and binary systems of dyes, and according to the negative values of standard entropy ΔS° shows that adsorption is made with increase in the order to the solid-solution interface [2] and that the dye molecules distribution order on the adsorbent is important compared to that in the solution. ΔG° increases with the increase in solution temperature for the two dyes in single and binary systems, which can be explained by the fact why adsorption becomes very difficult and underprivileged when the temperature becomes very high [40,41]. The positive values of ΔG° indicate that the adsorption of the treated dyes is not spontaneous and its increase with the temperature indicates an increase in the disorder during adsorption, the random aspect increases with the solid-solution interface during this adsorption process. This can be explained by the redistribution of energy between the adsorbent and adsorbat. In addition, the examination of the enthalpy ΔH° (<40 kJ/mol) shows that it is about a physical adsorption [42-44].

Conclusion

In this study the silica-chitosan composite was developed from the northern shrimp "Pandalus Borealis" and "Crangon-Crangon" for the adsorption of anionic dyes and particularly RR 23 and RB 19 in single and binary systems of dyes. The results showed that the Si-Cs composite can be effectively used as biosorbent for the removal of anionic dyes, this biosorbent showed a high adsorption capacity to RR 23 and RB 19 in single and binary systems of dyes.

The effect of operational parameters on the adsorption of RR 23 and RB 19 in single and binary systems of dyes such as the adsorbent dose, the pH, the initial dye concentration, the contact time and temperature were carried out in static mode. The experimental results showed that:

- The optimal adsorbent amounts for the elimination of RR 23 and RB 19 in single and binary system are 50mg in the single system and of 60mg in the binary system of dyes.
- The maximum dyes adsorption capacity occurred with pH 1 for the single and binary systems of dyes.
- The optimal dyes concentrations are equal to 125 mg/l and 200mg/l for RR 23 and RB 19 in the single system of dyes, respectively, and in the binary system the optimal dyes concentrations are 175mg/l and 225mg/l for RR 23 and RB 19 respectively.
- The optimal contact time for dyes adsorption RR 23 and RB 19 in the two systems single and binary is of 180 min.
- The maximum adsorption of RR 23 and RB 19 in both single and binary systems of dyes was obtained at 25°C.

Freundlich model described better the adsorption of RR23 and RB19 in single and binary systems of dyes, the pseudo-second-order model is the one that best describes the adsorption process of the two dyes in both systems, and according to the thermodynamic values we can conclude that the adsorption is not spontaneous and exothermic with an enthalpy ΔH° less than 40 kJ/mol shows that it is a physical adsorption.

References

1. El Fargani H., Lakhmiri R., Albourine A., Cherkaoui O., Safi M. *J. Mater. Environ. Sci.* 7 (4) (2016) 1334-1346.
2. Aarfane A., Salhi A., El Krati M., Tahiri S., Monkade M., Lhadi E .K., Bensitel M. *J. Mater. Environ. Sci.* 5 (6) (2014) 1927-1939.
3. Cardona E. Doctoral dissertation, (2015).
4. Laabd M., El Jaouhari A., Chafai H., Aarab N., Bazzaoui M., Albourine A. *J. Mater. Environ. Sci.* 6 (4) (2015) 1049-1059.
5. Kassale A., Barouni K., Bazzaoui M., Martins J., Albourine A. *prot. met. phys. chem. surf.* 51(3) (2015) 382-389.
6. Laabd M., El Jaouhari A., Bazzaoui M., Albourine A., Lakhmiri R. *IJERT.* 3(11) (2014) 224-231.
7. Namasivayam C., Radhika R., Suba S. *Waste. Manag.* 21 (2001) 381-387.
8. Budnyak T., Tertykh V., Yanovska E. *J. Mater. Sci.* 20(2) (2014) 177-182.
9. Younes I., Rinaudo M. *Mar. Drugs.* 13(3) (2015) 1133-1174.
10. Ospina N. M., Alvarez S. P. O., Sierra D. M. E., Vahos D. F. R., Ocampo P. A. Z., Orozco C.P.O. *J. Mater. Sci. Mater. Med.* 26(3) (2015) 1-9.
11. Kyzas G. Z., Sifaka P. I., Pavlidou E. G., Chrissafis K. J., Bikiaris D. N. *Chem. Eng. J.* 259 (2015) 438-448.
12. Gandhi M. R., Meenakshi S. *Int. J. Biol. Macromolec.* 50(3) (2012) 650-657.
13. Li F., Jiang H., Zhang S. *Talanta.* 71(4) (2007) 1487-1493.
14. Mahmoodi N. M., Masrouri O. *J. Solution. Chem.* 44(8) (2015) 1568-1583.
15. Choy K. K., Porter J. F., McKay G. *J. Chem. Eng. Data.* 45(4) (2000) 575-584.
16. Mahmoodi N.M., Salehi R., Arami M., Bahrami H. *DESALINATION.* 267(1) (2011) 64-72.
17. Yuan W. Z., Mao P. E. N. G., Yu Q. M., Tang B. Z., Zheng Q. *Chem. Res. Chin. Univ.* 22(6) (2006) 797-802.
18. Gandhi M. R., Kousalya G. N., Viswanathan N., Meenakshi S. *Carbohydr. Polym.* 83(3) (2011) 1082-1087.
19. Kousalya G. N., Gandhi M. R., Meenakshi S. *Int. J. Biol. Macromolec.* 47(2) (2010) 308-315.
20. Ogawa K., Hirano S., Miyaniishi T., Yui T., Watanabe T. *Macromolecules.* 17(4) (1984) 973-975.
21. Hou A., Chen H. *Mater. Sci. Eng., B.* 167(2) (2010) 124-128.
22. Crini G., Gimbert F., Robert C., Martel B., Adam O., Morin-Crini N., Badot P. M. *J. Hazard. Mater.* 153(1) (2008) 96-106.
23. Crini G., Badot P. M. *Prog. Polym. Sci.* 33(4) (2008) 399-447.

24. Chatterjee S., Chatterjee S., Chatterjee B. P., Das A. R., Guha A. K. *J. Colloid Interface Sci.* 288(1) (2005) 30-35.
25. Chiou M. S., Li H. Y. *Chemosphere.* 50(8) (2003) 1095-1105.
26. Langmuir I. *J. Am. Chem. Soc.* 38(11) (1916) 2221-2295.
27. Das S. K., Bhowal J., Das A. R., Guha A. K. *Langmuir.* 22(17) (2006) 7265-7272.
28. Choy K. K., Porter J. F., McKay G. *Chem. Eng. J.* 103(1) (2004) 133-145.
29. Dada A. O., Olalekan A. P., Olatunya A. M., Dada O. *J. appl. chem.* 3(1) (2012) 38-45.
30. Dubinin M. *Chem. Rev.* 60(2) (1960) 235-241.
31. Hobson J. P. *J. Phys. Chem.* 73(8) (1969) 2720-2727.
32. Yuh-Shan H. *Scientometrics.* 59(1) (2004) 171-177.
33. BENAMROUI F. Doctoral dissertation, (2015).
34. Ho Y. S., McKay G. *Process Biochem.* 34(5) (1999) 451-465.
35. Weber W. J., Morris J. C. *J. Sanit. Eng. Div.* 89(2) (1963) 31-60.
36. Ma J., Yu F., Zhou L., Jin L., Yang M., Luan J., Chen J. *ACS Appl. Mater. Interfaces.* 4(11) (2012) 5749-5760.
37. Lv L., He J., Wei M., Evans D. G., Duan X. *Water. Res.* 40(4) (2006) 735-743.
38. Belaid K. D., Kacha S. *Water. Sci. Rev.* 24(2) (2011) 131-144.
39. Çolak F., Atar N., Olgun A. *Chemical. Eng. J.* 150(1) (2009) 122-130.
40. Talidi A. Doctoral dissertation, (2006).
41. Namasivayam C., Senthilkumar S. *Ind. Eng. Chem. Res.* 37(12) (1998) 4816-4822.
42. Gherbi N. Doctoral dissertation, (2008).
43. Ahmad R., Kumar R. *Appl. Surf. Sci.* 257(5) (2010) 1628-1633.
44. Zhang Z., O'Hara I. M., Kent G. A., Doherty W. O. *Ind. Crops. Prod.* 42 (2013) 41-49.

(2017) ; <http://www.jmaterenvironsci.com>